First-principles studies of the atomic reconstructions of CdSe (001) and (111) surfaces

2009 J. Phys.: Condens. Matter 21 095001

(http://iopscience.iop.org/0953-8984/21/9/095001)

J. Phys.: Condens. Matter **21** (2009) 095001 (7pp) doi:10.1088/0953-8984/21/9/095001

First-principles studies of the atomic reconstructions of CdSe (001) and (111) surfaces

L Zhu[1,2,4], K L Yao[2,3,4], Z L Liu[2] and Y B Li[2]

[1] School of Optoelectronics Science and Engineering, Huazhong University of Science and Technology, Wuhan 430074, People's Republic of China
[2] School of Physics, Huazhong University of Science and Technology, Wuhan 430074, People's Republic of China
[3] International Center of Materials Physics, The Chinese Academy of Science, Shengyang 110015, People's Republic of China

E-mail: wl-zl41@163.com (L Zhu) and klyao@hust.edu.cn

Received 3 September 2008, in final form 10 December 2008
Published 20 January 2009
Online at stacks.iop.org/JPhysCM/21/095001

Abstract

We have performed the first-principles total-energy calculations to investigate (2 × 1), (1 × 2), (2 × 2), (4 × 2) and (2 × 4) reconstructions of Cd- and Se-terminated CdSe(001) and (111) surfaces as a function of the surface stoichiometry and the Cd chemical potential. We find that there exist Cd dimers on the (001) surface and Se tetramers on the (111) surface. Comparing surface formation energies as a function of the Cd chemical potential μ_{Cd}, we find the Cd-vacancy and Se-vacancy (2 × 2) structures to be energetically favorable for the Cd-terminated (001) surface at high μ_{Cd} and Se-terminated (001) surface at low μ_{Cd}, respectively. In contrast, an Se-tetramer (2 × 4) structure is more favorable than the vacancy structure for the Se-terminated CdSe(111) surface almost in the whole region of allowed μ_{Cd}.

(Some figures in this article are in colour only in the electronic version)

1. Introduction

II–VI semiconductors have drawn increasing interest in view of their potential applications in optoelectronic devices for detection and stimulated emission in the IR spectral region [1, 2]. More recently, there have been numerous studies focusing on the surface structure of small cadmium selenide (CdSe) semiconductor structures such as thin films, quantum dots and quantum wires [3–6]. CdSe films are of interest for their potential applications as photoconductors, solar cells, thin film transistors, gas sensors, photographic photoreceptors, etc [7–11]. Nanostructures of CdSe have also been demonstrated to be a promising II–VI semiconductor material for optoelectronic devices and biomedical fluorescent labels [12, 13]. CdSe nanocrystals have a wurtzite lattice structure under room conditions [14]. Previous studies found that the surface passivation plays a key role in the photoluminescence quantum yield of these quantum dots [12–14]. Bulk CdSe has two crystal structures: wurtzite (WZ, hexagonal) at atmospheric pressure and zinc blende (ZB, cubic) which generally forms in thin films. These structures only differ in the stacking sequence of the CdSe hexagonally packed layers. The ZB structure has an ABABAB stacking sequence along the [001] direction and an ABCABC stacking sequence along the [111] direction. The WZ structure has an ABABAB stacking sequence along the [0001] direction. The ground state energy difference between these two structures is small. ZB is the stable phase under room temperature, but it could transform reversibly to the WZ structure at a critical temperature of 95 ± 5 °C [15].

The knowledge of II–VI semiconductor atomic surface structure is important to improve passivation and for the tailoring of heterostructures. A number of experimental and theoretical investigations have been carried out on II–VI semiconductors and their surfaces [16–23]. In general, the non-polar (110) zincblende and (10$\bar{1}$0) wurtzite surfaces of II–VI compounds show an outward relaxation of the surface-layer anions and an inward relaxation of the surface-layer

[4] Authors to whom any correspondence should be addressed.

cations. Recently, there has been some work on studying the surface of the III–V and II–VI semiconductors, which found that the reconstructed surface consisted of various combinations of dimers [19, 24–29]. First-principles total-energy methods have been successfully applied to the study of the semiconductor surface reconstructions and provide a powerful tool for understanding the energetics of various defect formations and surface reconstructions [30–33]. In spite of the renewed experimental interest for the polar terminations of the II–VI semiconductors, no theoretical or experimental study of either the (001) or the (111) surface of CdSe bulk has been performed so far, to our knowledge. It is the aim of this work to analyze the electronic properties and the stability of these surfaces. In this paper, we have performed a systematic *ab initio* study comparing the dimer, tetramer and vacancy-type structures on the CdSe ZB-structure Cd- and Se-terminated (2 × 1), (1 × 2), (2 × 2), (4 × 2) and (2 × 4) (001) and (111) surfaces, and calculated the thermodynamical stability of various surface reconstructions as a function of Cd chemical potential μ_{Cd}. It is found that Cd dimers and Se tetramers are favored on some specific surfaces of CdSe, which is not found in previous studies. Comparing surface formation energies as a function of the Cd chemical potential μ_{Cd}, we find the Cd-vacancy and Se-vacancy (2 × 2) structures to be energetically favorable for the Cd-terminated (001) surface at high μ_{Cd} and the Se-terminated (001) surface at low μ_{Cd}, respectively. In contrast, an Se-tetramer (2 × 4) structure is more favorable than the vacancy structure for the Se-terminated CdSe(111) surface almost in the whole region of allowed μ_{Cd}.

2. Computational method

The calculations were performed using a first-principles full-potential augmented plane-wave (FP-APW) method in the WIEN2k package [34]. We have calculated the optimized lattice constants and the heat of formation of bulk ZB CdSe with the local density approximation (LDA) and generalized gradient approximation (GGA). The optimized lattice constant of the ZB CdSe with LDA is 6.018 Å [35], which is in good agreement with the experimental value of 6.052 Å, but that with GGA is 6.195 Å, which is about 2.4% larger than the experimental value. The heat of formation for CdSe bulk ΔH_{f} (CdSe) with the LDA method is 1.25 eV, which is a little lower than the experimentally determined value of 1.42 eV [36], but that with the GGA method is 1.34 eV, which is still a little lower than the experimental value. In order to get a more correct bond length of the surface, we have chosen the LDA to calculate the surface free energy and the bond length of the surfaces. The linearized augmented plane-waves basis set was used with $R_{\mathrm{Cd}}^{\mathrm{MT}} = 2.0$ au and $R_{\mathrm{Se}}^{\mathrm{MT}} = 1.5$ au. Inside the muffin tins (MTs) the wavefunctions are expanded in spherical harmonics up to $l_{\mathrm{max}}^{\mathrm{wf}} = 12$ and the nonspherical contributions to the electron density and potential are considered up to $l_{\mathrm{max}}^{\mathrm{pot}} = 6$. The charge density Fourier expansion cutoff $G_{\mathrm{max}} = 14$ in the muffin tins. Three hundred k-points in the first Brillouin zone were adopted in the calculations (250 points in the irreducible part of the surface Brillouin zone). The plane-wave cutoff energy is 296 eV. The self-consistency was achieved by demanding the convergence of the integrated charge difference between the last two iterations to be smaller than 1×10^{-4} e/cell. After the self-consistent calculations finished, the convergence of the total energies was checked to be smaller than 0.1 meV.

Table 1. The Cd-dimer bond length of the (001) surface. The Cd–Cd bond length of bulk is 4.255 Å.

Surface	The Cd-dimer bond length (Å)
CdSe(001)–8Cd (4 × 2)	2.693
CdSe(001)–6Cd (2 × 4)	2.904
CdSe(001)–4Cd (2 × 4)	2.700
CdSe(001)–2Se (2 × 4)	2.769

3. Results of surface calculations

3.1. Geometry optimization results

To simulate the surface, the slab geometry was used and the vacuum was also used in the simulations, the vacuum between the repeated slabs amounting to 10 Å. The slab comprised eight or nine Cd–Se layers, depending on the surface termination, each of which contained one Cd atomic layer and one Se atomic layer. The backside of the surface, which is not of interest, was terminated by fictitious H atoms to prevent the dangling-bond effect [37]. The top four atomic layers are allowed to relax until the forces are less than 0.01 eV $\mathrm{Å}^{-1}$, whilst the convergence of the total energies was checked to be smaller than 1.0×10^{-5} eV/atom. The computational methodology that we are using for periodic boundary conditions is based on the density function theory and the state of electrons is described by the plane wave. The plane wave expanded along the 10 Å vacuum between two supercells almost equals zero, so there is almost no coupling of the electrons in the two near supercells. So the dipole–dipole interactions of the two near supercells along the 10 Å vacuum are very small in the density function theory, and the 10 Å vacuum gap is sufficient to prevent such significant interactions

After optimization, it is found that there exist Cd dimers of the (001) surface and Se tetramers of the (111) surface. The side views of the different ZB-structure CdSe(001) and (111) Cd-terminated and Se-terminated (4 × 2), (2 × 4) and (2 × 2) surface dimerization, tetramer and reconstruction models were presented in figure 1, which only shows the outermost five atomic layers and some more stable surfaces. After analysis, it is found that the dimers of the Cd-terminated (001) surface come from the outermost Cd atoms along the y direction, and those of the Se-terminated (001) surfaces with Se vacancy come from the second-layer Cd atoms, but there are no dimers of the outermost Se atom. The bonding distances of the dimer Cd–Cd are shown in table 1, which are much smaller than those of bulk (Cd–Cd: 4.255 Å). It is found that there exist the outermost Cd dimerization on the CdSe(001)–8Cd (4 × 2), CdSe(001)–6Cd (2 × 4), CdSe(001)–4Cd (2 × 4) and CdSe(001)–2Se (2 × 4) surfaces. The surface Cd atoms of CdSe(001)–8Cd (4 × 2), CdSe(001)–6Cd (2 × 4), CdSe(001)–4Cd (2 × 4), CdSe(001)–2Cd (4 × 2) and CdSe(001)–2Cd

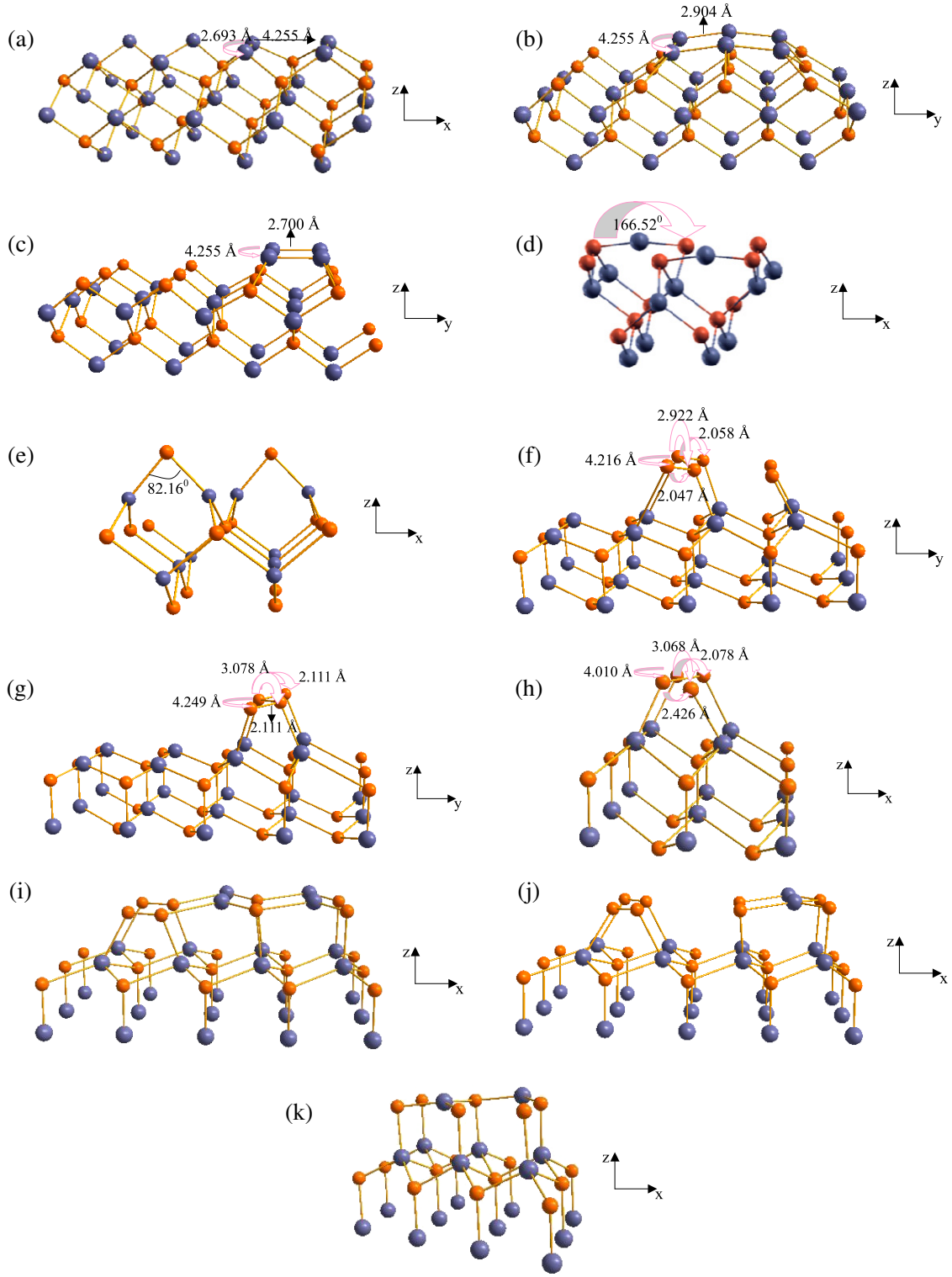

Figure 1. Side view of dimerization, tetramers and reconstruction (001) and (111) layer slabs of ZB-structure CdSe: ((a)–(e) belong to CdSe(001) surface and (f)–(k) belong to CdSe(111) surface). Se (small sphere) and Cd (large sphere) atoms. (a) CdSe(001)–8Cd (4 × 2), (b) CdSe(001)–6Cd (2 × 4), (c) CdSe(001)–4Cd (2 × 4), (d) CdSe(001)–2Cd (2 × 2), (e) CdSe(001)–2Se (2 × 2), (f) CdSe(111)–6Se (2 × 4), (g) CdSe(111)–4Se (2 × 4), (h) CdSe(111)–4Se (2 × 2), (i) CdSe(111)–4Cd (4 × 2), (j) CdSe(111)–2Cd (4 × 2), (k) CdSe(111)–2Cd (2 × 2).

(2 × 2) surfaces relax towards the second-layer Se atoms, and the surface Cd atoms and the second-layer Se atoms on the CdSe(001)–2Cd (4 × 2), CdSe(001)–6Cd (2 × 4) and CdSe(001)–2Cd (2 × 2) surfaces form a very flat plane. There exist the outermost Se tetramers on the (111) surface, which are CdSe(111)–8Se(2 × 4), CdSe(111)–6Se (2 × 4), CdSe(111)–4Se (2 × 4), CdSe(111)–4Se (2 × 2), CdSe(111)–4Cd (4 × 2) and CdSe(111)–2Cd (4 × 2) surfaces. The tetramers of the Se-terminated (111) surface come from the outermost Se atoms and these of the Cd-terminated structures with Cd vacancy

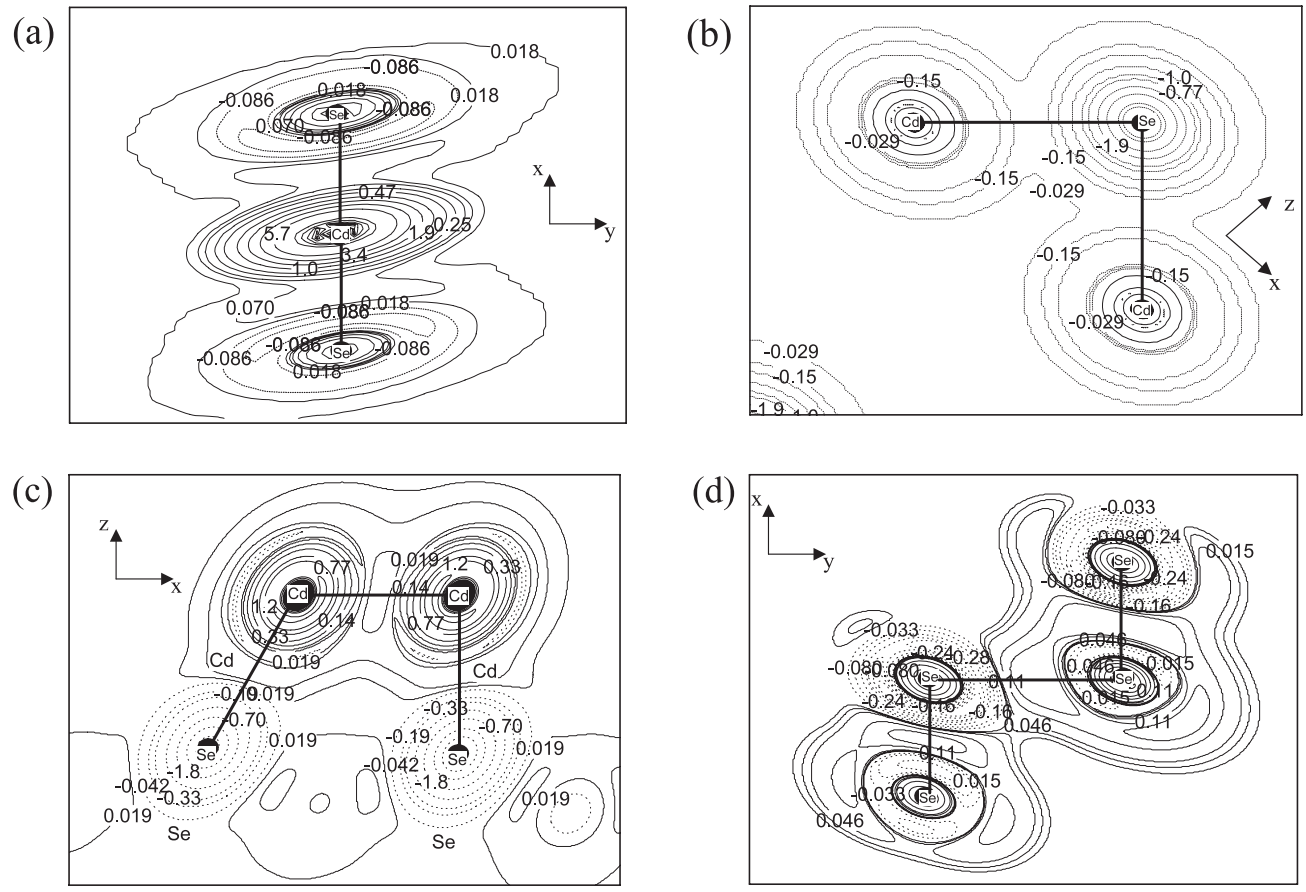

Figure 2. The difference charge density contour plots for ZB-structure CdSe (001) and (111) surface: (a) for CdSe(001)–2Cd (2 × 2); (b) for CdSe(001)–2Se (2 × 2); (c) for CdSe(001)–8Cd (4 × 2); (d) for CdSe(111)–8Se (2 × 4). The negative densities in a given region imply that the electron density has been transferred from that region.

come from the second-layer Se atoms, but there is no dimer or tetramer for the outermost Cd atom. The shortest bonding distances of the tetramer Se–Se are shown in table 2. The surface Cd atoms on the CdSe(111)–4Cd (4 × 2), CdSe(111)–2Cd (4×2), CdSe(111)–2Cd (4×2) and CdSe(111)–2Cd (2×2) surfaces relax towards the second-layer Se atoms; the surface Cd atoms and the second-layer Se atoms on CdSe(111)–2Cd (4 × 2) and CdSe(111)–2Cd (2 × 2) surfaces form a very flat plane. Except for these dimers and tetramers, none of the other dimers or tetramers is found on the surfaces which we have considered. The simulation and calculation results show that, in the ZB structure of CdSe, the anions (Se) and cations (Cd) of (001) surfaces have an outward and inward relaxation of the first layer respectively, except for CdSe(001)–6Cd (4 × 2) and CdSe(001)–4Cd (2 × 2) surfaces, as is shown in table 3. But some of the Cd atoms in the CdSe(111) surface move in, as is shown in the above discussion, and the others move out. Recent experimental and theoretical results revealed that in both the CdSe non-polar $(10\bar{1}0)$ and $(11\bar{2}0)$ surfaces there is a relaxation outward of the anions (Se) and an inward (Cd) relaxation of the first layer [20, 31, 38, 39]. It is found that the qualitative features of the relaxation in nanostructural and bulk surfaces are similar [9, 10, 40]. The simulations of nanocrystals CdSe surface predict a large reconstruction of these CdSe nanoparticle faces, including a Cd–Se dimer rotation into the surface [10]. The reconstructions, dimers and tetramers of the surface atoms could improve the surface passivation, which was 'self-healing' the surface electronic structure, resulting in the opening of an optical gap in CdSe films and quantum dots.

Table 2. The Se-tetramer shortest bond length of the (111) surface. The Se–Se bond length of the bulk is 4.255 Å.

Surface	Se-tetramer shortest bond length (Å)
CdSe(111)–8Se (2 × 4)	2.464
CdSe(111)–6Se (2 × 4)	2.047
CdSe(111)–4Se (2 × 4)	2.103
CdSe(111)–4Se (2 × 2)	2.073
CdSe(111)–4Cd (4 × 2)	2.037
CdSe(111)–2Cd (4 × 2)	1.923

3.2. The difference charge density

For an II–VI semiconductor such as CdSe, each cation has two valence electrons and each anion has six valence electrons. Thus, on average, each atomic orbital contributes $\frac{1}{2}$ or $\frac{3}{2}$ electrons to each bond in the ZB structure. Thus there are one (i.e. $2 \times \frac{1}{2}$) or three (i.e. $2 \times \frac{3}{2}$) electrons in the two

Table 3. Interplanar distances and rumpling on CdSe stoichiometric (001) and (111) terminations for the outermost two layer atoms. Positions of crystal planes are computed by averaging the coordinates of the corresponding atoms. The interplanar distances are given in ångströms and their variations with respect to the bulk value are provided in parentheses (in per cents of interplanar distances in the bulk). A positive sign corresponds to outward atomic displacements (toward the vacuum). Rumpling is determined as the distance between the atom and the respective crystal plane.

Layer	Interplanar distances (Å)	Rumpling (Å)
CdSe(001)–8Cd (4 × 2)	Cd–Se: 1.469(−2.37%)	Cd: −0.140, Se: −0.059
CdSe(001)–6Cd (4 × 2)	Cd–Se: 1.205(−19.93%)	Cd: −0.373, Se: −0.033
CdSe(001)–4Cd (4 × 2)	Cd–Se: 1.383(−8.06%)	Cd: −0.171, Se: −0.031
CdSe(001)–2Cd (4 × 2)	Cd–Se: 1.369(−8.99%)	Cd: −0.174, Se: −0.038
CdSe(001)–4Cd (2 × 2)	Cd–Se: 1.695(+12.67%)	Cd: +0.393, Se: +0.202
CdSe(001)–2Cd (2 × 2)	Cd–Se: 0.283(−81.17%)	Cd: −0.836, Se: +0.385
CdSe(001)–8Se (2 × 4)	Se–Cd: 1.345(−10.58%)	Se: +0.027, Cd: +0.174
CdSe(001)–6Se (2 × 4)	Se–Cd: 1.557(+3.5%)	Se: +0.24, Cd: −0.027
CdSe(001)–4Se (2 × 4)	Se–Cd: 2.056(+36.68%)	Se: +0.660, Cd: +0.108
CdSe(001)–2Se (2 × 4)	Se–Cd: 2.035(+35.29%)	Se: +0.592, Cd: +0.061
CdSe(001)–4Se (2 × 2)	Se–Cd: 1.400(−6.92%)	Se: +0.001, Cd: +0.103
CdSe(001)–2Se (2 × 2)	Se–Cd: 1.897(+26.07%)	Se: +0.441, Cd: +0.048
CdSe(111)–8Cd (4 × 2)	Cd–Se: 0.889(+2.32%)	Cd: +0.522, Se: +0.502
CdSe(111)–6Cd (4 × 2)	Cd–Se: 0.404(−53.13%)	Cd: −0.189, Se: +0.272
CdSe(111)–4Cd (4 × 2)	Cd–Se: 0.290(−66.58%)	Cd: −0.304, Se: +0.274
CdSe(111)–2Cd (4 × 2)	Cd–Se: 0.343(−60.56%)	Cd: −0.462, Se: +0.064
CdSe(111)–4Cd (2 × 2)	Cd–Se: 0.857(−1.34%)	Cd: +0.241, Se: +0.252
CdSe(111)–2Cd (2 × 2)	Cd–Se: 0.238(−72.62%)	Cd: −0.365, Se: +0.266
CdSe(111)–8Se (2 × 4)	Se–Cd: 2.546(−2.28%)	Se: +0.267, Cd: +0.246
CdSe(111)–6Se (2 × 4)	Se–Cd: 3112(+19.43%)	Se: +0.478, Cd: −0.021
CdSe(111)–4Se (2 × 4)	Se–Cd: 2.748(+5.45%)	Se: +0.475, Cd: +0.333
CdSe(111)–2Se (2 × 4)	Se–Cd: 2.957(+13.47%)	Se: +0.286, Cd: −0.065
CdSe(111)–4Se (2 × 2)	Se–Cd: 2.759(+5.89%)	Se: +0.358, Cd: +0.201
CdSe(111)–2Se (2 × 2)	Se–Cd: 2.991(+14.76%)	Se: +0.289, Cd: −0.095

dangling bonds per cation or anion on the ideal (1 × 1) cation- or anion-terminated (001) and (111) surfaces. In order to understand how the charge build-up on the bonds of the surface originates, we plot the difference charge density contours in figure 2, where the difference charge density is defined as the difference between the total charge density of the solid and a superposition of atomic charge. The dotted line represents the negative densities, and the negative densities in a given region imply that the electron density has been transferred from that region. For the Cd-vacancy structure on the CdSe (2 × 2) (001) and (111) surfaces, the electrons in the dangling bonds of the surface Cd atoms are transferred into the dangling bonds of the second-layer Se atoms. The surface Cd atoms relax towards the second-layer Se atoms; the surface Cd atoms and the second-layer Se atoms form a very flat plane, which is also shown in figures 1(d) and (k). The Se–Cd–Se bond angle at the Cd-vacancy (2 × 2) (001) surface becomes nearly 180°. This finding reveals that these Cd and Se atoms mainly form sp-like bonds and the structure is stabilized by the formation of these bonds. The sp-like bond formation of Cd-vacancy structure on the CdSe (2 × 2) (001) surface was confirmed by investigating the difference charge density distribution. The difference charge density for the Cd-vacancy (2 × 2) (001) structure is shown in figure 2(a). The figure is plotted in a plane which contains a surface Cd atom and two second-layer Se atoms. The electron density is similar to that of the Zn-vacancy structure on the ZnSe(100) and the Ga-vacancy structure on the GaAs(100) surface [24, 25]. The electrons around the relaxed Cd atoms form an sp type of hybridization. The sum of the three bond angles around the surface Cd atoms at the Cd-vacancy (2×2) (111) surface is 357° (figure 1(k)), which shows that the surface Cd atoms mainly make sp^2-like bonds with Se atoms. The Cd–Se bond length at the Cd-vacancy (2 × 2) (001) surface is 2.44 Å, compressed by 6.2% compared to the ideal bulk distance. The reduction of the bond length occurs as a result of the charge transfer and reduced coordination of the cation [41]. For the case of the Se-vacancy (2 × 2) structure, the electrons in the dangling bonds of the Cd atoms in the second layer are transferred to the dangling bonds of the Se atoms in the surface layer and fill the dangling-bond states of the Se atoms. The extra electrons around the Se atoms of the Se-vacancy (2 × 2) (001) surface is found to reduce the Cd–Se–Cd angle to 82.16°, which is appreciably smaller than the ideal bond angle of 109.47° in the ZB structure, as is shown in figure 1(e). The Se–Cd bond length at the Se-vacancy (001) surface is reduced to 2.51 Å, which is about 96.3% of its bulk bond length value. The difference charge density contour plot for the Se-vacancy structure on the CdSe (2×2) (001) surface is shown in figure 2(b). The Se–Cd bond length at the Se-vacancy (111) surface is reduced to 95.9% of its bulk bond length value, and it is 2.50 Å. The shrinking of the bond length is due to the charge transfer between the atoms. The similar displacement of these layers has also been found by Park for ZnSe [24]. Recent experimental and theoretical results revealed that both the non-polar CdSe $(10\bar{1}0)$ and $(11\bar{2}0)$ surfaces exhibit nearly bond-length-conserving relaxations to achieve local hybridization from sp^3 to p^3 for the anions (Se) and sp^2 for the cations (Cd) [20, 38, 39]. The simulations of the CdSe nanocrystals' surface predict the surface cations (Cd) show a preference to form sp^2-like bonds with their three nearest anion (Se)

neighbors [9, 10, 40], which is similar to the result of the ZB-structure CdSe(111) surface in our studies.

The contours in figure 2(c) describe the difference charge density for the Cd dimer. This figure is plotted in a plane which contains two surface Cd atoms and two second-layer Se atoms. Between the Cd atoms in the top layer, the valence charge is localized and clearly shows the bond formation between these atoms. For Se tetramers of the CdSe(111) surface, the atomic geometry is completely different from that of the ideal bulk surface, which is evidently shown in the difference charge density contour plot in figure 2(d). The Se–$Se_{surface}$ bond distance is shorter than the Se–Se_{inner} bond distance of the bulk materials, which favors stronger binding of these states.

3.3. Chemical potential results

Since these surfaces are all polar, theoretical determination of their atomic structures generally requires the calculation of minimum-energy geometries as a function of Cd or Se coverage, or equivalently as a function of Cd or Se chemical potentials. The surface energies were calculated from the total energies of the respective slabs using a scheme introduced by Qian *et al* [26]. The surface energy σ was computed from the formula

$$\sigma = E_{\rm tot} - 0.5(n_{\rm Cd} + n_{\rm Se})\mu^{\rm bulk}_{\rm CdSe} - 0.5(n_{\rm Cd} - n_{\rm Se}) \times (\mu^{\rm bulk}_{\rm Cd} - \mu^{\rm bulk}_{\rm Se}) - 0.5(n_{\rm Cd} - n_{\rm Se})\Delta\mu, \quad (1)$$

where

$$\Delta\mu = (\mu_{\rm Cd} - \mu^{\rm bulk}_{\rm Cd}) - (\mu_{\rm Se} - \mu^{\rm bulk}_{\rm Se}). \quad (2)$$

Here n denotes the number of atoms of the respective species within the supercell and μ denotes the respective chemical potential. The superscript 'bulk' refers to the chemical potential of the elementary bulk material referred to in the subscript. The chemical potentials of bulk Cd and bulk Se were calculated self-consistently by optimizing their respective supercell geometries until the minimum of the total energy was reached. Calculating from these data the heat of formation for CdSe bulk $\Delta H_{\rm f}$ (CdSe) we found a value of 1.25 eV, which is a little lower than the experimentally determined value of 1.42 eV [36]. In the above expression for σ, $\Delta\mu$ extends over the interval $-\Delta H_{\rm f} < \Delta\mu < \Delta H_{\rm f}$. Since this formula is symmetric with respect to the chemical potentials of the two constituents, we expect that it will minimize the error arising from the difference between the self-consistently calculated value for $\mu^{\rm bulk}_{\rm CdSe}$ and that taken from the literature.

The surface energies of these surfaces are plotted in figure 3 ((a) for (001) and (b) for (111) surfaces) against the variable $\Delta\mu$, as defined in equation (2). Enclosed within the dashed lines is the interval given by the self-consistently determined value for the heat of formation of bulk CdSe. The abscissa extends towards lower values as far as −1.42 eV and to higher ones as far as 1.42 eV, the experimental value for $\Delta H_{\rm f}$ (CdSe). Figure 3(a) shows that only two types of structures are energetically favorable among the considered structures. The Se-vacancy (2 × 2) structure is favorable in the region of low $\mu_{\rm Cd}$, i.e. Se-rich condition, while the Cd-vacancy (2 × 2) structure is favorable in the region of high $\mu_{\rm Cd}$, i.e. Cd-rich

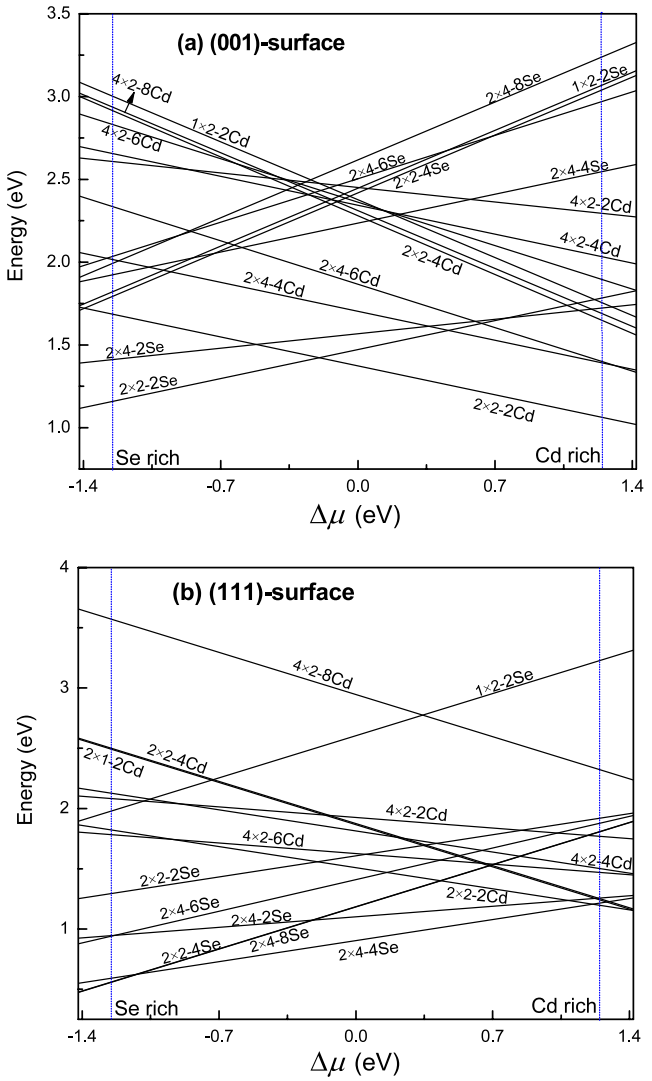

Figure 3. Surface formation energies per (1 × 1) unit cell for CdSe (a) (001) and (b) (111) surfaces as a function of $\mu_{\rm Cd}$.

condition. Our result is similar to that found by Park [24] and Gundel [26], but for the CdSe(001) surface we do not find the Se dimerization, but the dimerization and vacancy have greatly lowered the surface energy. As discussed earlier, for the Cd-vacancy (2 × 2) structure, the electrons around the surface Cd atoms form sp-type hybridization. The energy reduction by this type of hybridization makes the Cd-vacancy structure relatively more stable than the Cd-dimer structure. From figure 3(b) it can be found that the Cd-vacancy (2 × 2) structure is favorable in the region of high $\mu_{\rm Cd}$, the Se tetramers 2 × 4 and 2 × 2 without Se-vacancy surface are favorable in the region of low $\mu_{\rm Cd}$ and the surface energy of the Se-tetramer 2 × 4 structure is lower than that of the Se-tetramer 2 × 2 structure: the difference is about 0.003 eV/(1 × 1). For the Se-terminated (111) surface, the $Se_{surface}$ atoms in the vacancy-terminated surface have many dangling-bond states, which makes the vacancy formation unfavorable relative to the tetramer formation. The surface energy of the Cd-vacancy (001) (2 × 2) structure is 1.0184 eV/(1 × 1) ($\Delta H_{\rm f}$ = 1.42 eV, experimentally) or 1.0609 eV/(1 × 1) ($\Delta H_{\rm f}$ = 1.25 eV, theoretically) in the

region of high μ_{Cd}. The surface energy of the Cd-vacancy (111) (2 × 2) structure is 1.1534 eV/(1 × 1) ($\Delta H_f = 1.42$ eV, experimentally) or 1.1959 eV/(1 × 1) ($\Delta H_f = 1.25$ eV, theoretically) in the region of high μ_{Cd}. The surface energy of the Cd-vacancy (001) (2 × 2) structure is lower than that of the Cd-vacancy (111) (2 × 2) structure, which is induced by the different hybridization of the surface Cd atoms. As is mentioned earlier, for the Cd-vacancy (001)-(2 × 2) structure, the $Cd_{surface}$ atoms are mainly sp hybridized, but in the Cd-vacancy (111)-(2 × 2) structure, the surface Cd atoms are mainly sp^2 hybridized, and generally sp-type hybridization is more stable than sp^2-type hybridization, which induces a Cd-vacancy (001)-(2 × 2) structure with a little lower surface energy than that of the Cd-vacancy (111)-(2 × 2) structure. After analysis, it is found that the dimerization, tetramer and vacancy relaxation could lower much of the surface energy.

4. Conclusions

We have performed *ab initio* calculations by the density-functional theory (DFT) with the LDA approach to investigate the structure of CdSe (001) and (111) Cd- and Se-terminated (2 × 1), (1 × 2), (2 × 2), (4 × 2) and (2 × 4) surfaces which consist of various combinations of dimers, tetramers and vacancies, and compared the surface energies as a function of the chemical potential of the Cd reservoir. According to our calculations, it is found that there exist Cd dimers on the (001) surface and Se tetramers on the (111) surface. The Cd-vacancy (2 × 2) structure is found to be energetically more favorable than the dimer structure for the Cd-terminated (001) surface, while the Se-vacancy (2 × 2) (001) structure is favorable in the region of low μ_{Cd}. The Cd-vacancy (2 × 2) (111) structure is favorable in the region of high μ_{Cd}, while the Se-tetramer (2 × 4) and (2 × 2) (111) surfaces are favorable in the region of low μ_{Cd}.

Acknowledgments

This work was supported by the National Natural Science Foundation of China under grant nos. 10574047, 10574048 and 20490210. This work was also supported by the National 973 Project under grant no. 2006CB921605.

References

[1] Jain M (ed) 1993 *II–VI Semiconductor Compounds* (Singapore: World Scientific)
[2] Birkmire R W and Eser E 1997 *Annu. Rev. Mater. Sci.* **27** 625
[3] Alivisatos A P 1996 *J. Phys. Chem.* **100** 13226
[4] Yu M, Fernando G W, Li R, Papadimitrakopoulos F, Shi N and Ramprasad R 2006 *Appl. Phys. Lett.* **88** 231910
[5] Puzder A, Williamson A J, Gygi F and Galli G 2004 *Phys. Rev. Lett.* **92** 217401
[6] Xi L f, Lam Y M, Xu Y P and Li L J 2008 *J. Colloid Interface Sci.* **320** 491–500
[7] Velumani S, Narayandass S K and Mangalaraj D 1998 *Semicond. Sci. Technol.* **13** 1016–24
[8] Smyntyna V A, Gerasutenko V, Kashulis S, Mattogno G and Reghini S 1994 *Sensors Actuators* B **19** 464
[9] Luo H, Samarth N, Zhang F C, Pareek A, Dobrowolska M, Mahalingam K, Otsuka N, Chou W C, Petrou A and Quadir S B 1991 *Appl. Phys. Lett.* **58** 1783
[10] Shizuo F, Wu Y-H, Yoichi K and Shigeo F 1992 *J. Appl. Phys.* **72** 5233
[11] Chiaa C H, Yuan C T, Ku J T, Yang S L, Chou W C, Juang J Y, Hsieh S Y, Chiu K C, Hsu J S and Jeng S Y 2008 *J. Lumin.* **128** 123–8
[12] Ledentsov N N, Krestnikov I L, Maximov M V, Ivanov S V, Sorokin S L, Kop'ev P S, Alferov Z I, Bimberg D and Sotomayor Torres C M 1996 *Appl. Phys. Lett.* **69** 1343
[13] Du G H, Liu Z L, Lu Q H, Xia X, Jia L H, Yao K L, Chu Q and Zhang S M 2006 *Nanotechnology* **17** 2850–4
[14] Shiang J J, Kadavanich A V, Grubbs R K and Alivisatos A P 1995 *J. Phys. Chem.* **99** 17417
[15] Fedorov V A, Ganshin V A and Korkishko Y N 1991 *Phys. Status Solidi* a **126** K5
[16] Zakharov O, Rubio A, Blase X, Cohen M L and Louie S G 1994 *Phys. Rev.* B **50** 10780
[17] Vogel D, Krüger P and Pollmann J 1996 *Phys. Rev.* B **54–58** 5495
[18] Schroer P, Kruger P and Pollmann J 1993 *Phys. Rev.* B **48** 18264
[19] Lin C-M, Tsai M-H, Yang T J and Chuu D S 1997 *Phys. Rev.* B **59** 9209
[20] Plucinski L, Johnson R L, Fleszar A, Hanke W, Weigand W, Kumpf C, Heske C, Umbach E, Schallenberg T and Molenkamp L W 2004 *Phys. Rev.* B **70** 125308
[21] Csik I, Russo S P and Mulvaney P 2005 *Chem. Phys. Lett.* **414** 322–5
[22] Ebina A, Asano K and Takahashi T 1980 *Phys. Rev.* B **22** 1980
[23] Yu W, Sullivan J L and Saied S O 1996 *Surf. Sci.* **352–354** 781–7
[24] Northrup J E and Froyen S 1993 *Phys. Rev. Lett.* **71** 2276
[25] Park C H and Chadi D J 1994 *Phys. Rev.* B **49** 16467
[26] Qian G, Martin R M and Chadi D J 1988 *Phys. Rev.* B **38** 7649
[27] Gundel S, Fleszar A, Faschinger W and Hanke W 1999 *Phys. Rev.* B **59** 15261
[28] Miyamoto Y and Nonoyama S 1992 *Phys. Rev.* B **46** 6915
[29] Ohna T 1993 *Phys. Rev. Lett.* **70** 631
[30] Brommer K D, Needels M, Larson B E and Joannopoulos J D 1992 *Phys. Rev. Lett.* **68** 1355
[31] Vogel D, Krüger P and Pollmann J 1998 *Surf. Sci.* **402–404** 774–7
[32] Taguchi A and Shiraishi K 2005 *Phys. Rev.* B **71** 035349
[33] Csik I, Russo S P and Mulvaney P 2005 *Chem. Phys. Lett.* **414** 322–5
[34] Blaha P, Schwarz K, Georg K, Madsen H, Kvasnicka D and Luitz J 2001 *Computer code WIEN2K* Techn. Universit. Wien, Austria
[35] Madelung O, Schulz M and Weiss H (ed) 1984 *Landolt-Börnstein Tables* vol 17a (Berlin: Springer) and references therein
[36] Goldfinger P and Jeunehomme M 1963 *Trans. Faraday Soc.* **59** 2851
[37] Shiraishi K 1990 *J. Phys. Soc. Japan* **59** 3455
[38] Duke C B and Yang Y R 1988 *J. Vac. Sci. Technol.* **6** 1440
[39] Horsky T N, Brandes G R, Canter K F, Duke C B, Horng S F, Kahn A, Lessor D L, Mills A P, Paton A, Stevens K and Stiles K 1989 *Phys. Rev. Lett.* **62** 1876
[40] Manna L, Wang L W, Cingolani R and Alvisatos A P 2005 *J. Phys. Chem.* B **109** 6183
[41] Kittel C 1986 *Introduction to Solid State Physics* 6th edn (New York: Wiley) p 77